



## NIH PUBLIC ACCESS

## Author Manuscript

*Acc Chem Res.* Author manuscript; available in PMC 2014 September 08.

Published in final edited form as:

*Acc Chem Res.* 2011 October 18; 44(10): 990–998. doi:10.1021/ar2000315.

## PRINT: A Novel Platform Toward Shape and Size Specific Nanoparticle Theranostics

JILLIAN L. PERRY, KEVIN P. HERLIHY, MARY E. NAPIER, and JOSEPH M. DESIMONE

Department of Chemistry, University of North Carolina at Chapel Hill, Chapel Hill, North Carolina 27599, United States

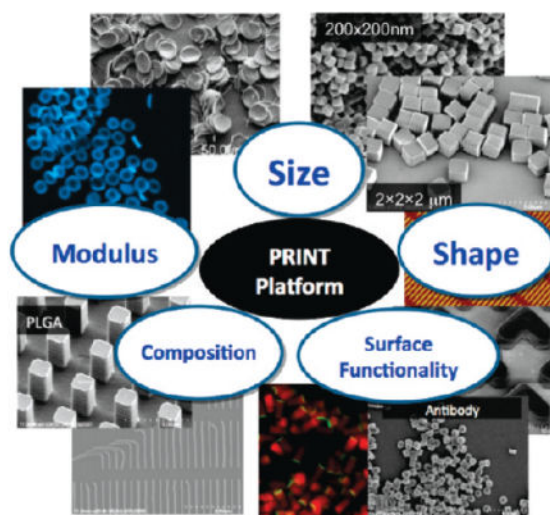
### CONSPECTUS

Nanotheranostics represents the next generation of medicine, fusing nanotechnology, therapeutics, and diagnostics. By integrating therapeutic and imaging agents into one nanoparticle, this new treatment strategy has the potential not only to detect and diagnose disease but also to treat and monitor the therapeutic response. This capability could have a profound impact in both the research setting as well as in a clinical setting. In the research setting, such a capability will allow research scientists to rapidly assess the performance of new therapeutics in an effort to iterate their designs for increased therapeutic index and efficacy. In the clinical setting, theranostics offers the ability to determine whether patients enrolling in clinical trials are responding, or are expected to respond, to a given therapy based on the hypothesis associated with the biological mechanisms being tested. If not, patients can be more quickly removed from the clinical trial and shifted to other therapeutic options. To be effective, these theranostic agents must be highly site specific. Optimally, they will carry relevant cargo, demonstrate controlled release of that cargo, and include imaging probes with a high signal-to-noise ratio.

There are many biological barriers in the human body that challenge the efficacy of nanoparticle delivery vehicles. These barriers include, but are not limited to, the walls of blood vessels, the physical entrapment of particles in organs, and the removal of particles by phagocytic cells. The rapid clearance of circulating particles during systemic delivery is a major challenge; current research seeks to define key design parameters that govern the performance of nanocarriers, such as size, surface chemistry, elasticity, and shape. The effect of particle size and surface chemistry on in vivo biodistribution of nanocarriers has been extensively studied, and general guidelines have been established. Recently it has been documented that shape and elasticity can have a profound effect on the behavior of delivery vehicles. Thus, having the ability to independently control shape, size, matrix, surface chemistry, and modulus is crucial for designing successful delivery agents.

In this Account, we describe the use of particle replication in nonwetting templates (PRINT) to fabricate shape- and size-specific microparticles and nanoparticles. A particular strength of the PRINT method is that it affords precise control over shape, size, surface chemistry, and modulus. We have demonstrated the loading of PRINT particles with chemotherapeutics, magnetic resonance contrast agents, and fluorophores. The surface properties of the PRINT particles can be

easily modified with “stealth” poly(ethylene glycol) chains to increase blood circulation time, with targeting moieties for targeted delivery or with radiolabels for nuclear imaging. These particles have tremendous potential for applications in nanomedicine and diagnostics.



## 1. Introduction

In 1965, Gordon Moore described the trend that the number of components in integrated circuits had approximately doubled every year since 1958. This trend has continued today, enabled by advances in photolithography which has taken the minimum feature size of transistors down from about 10  $\mu\text{m}$  in 1970 to 0.045  $\mu\text{m}$  today. In biological terms, this corresponds to going from the size of a red blood cell down to the size of a single virus particle. For the first time, the top-down nanofabrication technology from the semiconductor industry is in the size range to be relevant for the design of particle-based technologies including vaccines, medicines, and imaging agents. Herein we discuss a novel platform useful for the fabrication of shape and size specific theranostic agents using a particle nanofabrication technology known as particle replication in nonwetting templates (PRINT).

Nanoparticles have been extensively evaluated for both imaging and drug delivery; however, recent efforts have been focused on integrating therapeutic agents and imaging probes into one nanoparticle. Drug delivery and molecular imaging have benefited from advances in nanotechnology. Nanoparticles are now used for real-time molecularly targeted biomedical imaging and as nanotherapeutic agents.<sup>1–4</sup> This next generation of medical tools based upon the fusion of therapeutics and diagnostics has been termed theranostics. Using this treatment strategy, results of diagnostic tests can be used to design the appropriate targeted therapy as well as monitor the treatment response. In order to improve the efficacy of treatment and imaging, theranostic particles need to be biocompatible, monodisperse, and highly site-specific with optimal capability to carry relevant cargo, demonstrate controlled release of that cargo, and include imaging probes that give a high signal-to-noise ratio.

In the past 20 years, a plethora of nanoparticle delivery systems have been developed from a diverse array of materials ranging in size from a few tens of nanometers up to a few

micrometers; these delivery systems include but are not limited to liposomes, micelles, dendrimers, and polymer particles.<sup>5–13</sup> The utilization of nanocarriers for the delivery of therapeutics has led to a significant decrease in the toxicity of chemotherapeutics in clinical trials, which highlights the potential that nanoparticle based drug delivery can have on the improvement of cancer treatment and patient outcomes.<sup>14–16</sup>

There are many biological barriers in the human body that challenge the efficacy of nanoparticle delivery vehicles. Examples of these barriers include blood vessel walls, physical entrapment of the particles in organs, and removal by phagocytic cells. The rapid clearance of circulating particles during systemic delivery is a major challenge, and research is being conducted in an effort to define key design parameters that govern the performance of nanocarriers, such as size, surface chemistry, modulus, and shape. The effect of particle size and surface chemistry on in vivo biodistribution of nanocarriers has been extensively studied, and general guidelines have been established; however, literature guidelines pertaining to the effect of modulus and shape are lacking.<sup>17–23</sup> Clearance of particles from circulation is primarily due to opsonization, a process of protein adsorption that begins immediately after the particle comes in contact with plasma, the nature and conformation of the adsorbed proteins dictates the body's reaction.<sup>18</sup> In an effort to limit opsonization, surface modification of particles with poly-(ethylene glycol) (PEG) can help the particles evade the reticuloendothelial system which leads to extended circulation times.<sup>17,18,24</sup> Surface modifications with targeting ligands are also commonly used to target particles to various organs and pathological sites to increase drug delivery efficacy.<sup>25,26</sup> Discher and colleagues recently illustrated the dramatic role that size and modulus can play in nanocarrier function. They reported that flexible filamentous micelles with single dimensions as long as 8  $\mu\text{m}$  exhibited circulation half-lives of 5 days, which is significantly longer than that of PEGylated “stealth” spherical liposomes; however, outside of this effort, the effect of carrier modulus is essentially unexplored.<sup>21</sup>

Only in the past few years have researchers begun to illustrate the profound effect that shape can have on cellular internalization, circulation half-life, and biodistribution.<sup>22,27–29</sup> Decuzzi, Ferrari, and co-workers have demonstrated through mathematical models that the shape of carriers traveling through the blood vessels plays an important role in their margination toward the vessel wall.<sup>30,31</sup> They have also demonstrated using theoretical models that discoidal particles can drift laterally toward the blood vessel wall and can therefore adhere more strongly to the vascular walls under flow than spherical particles. Studies have also reported on higher targeting efficiency of nonspherical particles compared to their spherical counterparts.<sup>29,32</sup> Moreover, elongated particles can more effectively evade internalization by cells of different types as well as frustrate phagocytosis.<sup>33</sup> Collectively, these studies demonstrate that variation in particle shape can dramatically affect biodistribution and consequently the therapeutic efficacy or imaging efficiency.

## PRINT

PRINT is a top-down nanofabrication approach capable of generating monodisperse micro- and nanoparticles with well-defined size, shape, and modulus. The PRINT process has been described previously, and a schematic is illustrated in Figure 1.<sup>8,34–36</sup> Using this method, we

have fabricated a diverse array of particles ranging from 80 nm to 20  $\mu\text{m}$ , composed of poly(D-lactic acid) (PLA), PEG hydrogels, and proteins.<sup>35–37</sup> We have also demonstrated the fabrication of stimuli responsive particles fabricated with either disulfide or silyl ether cross-links.<sup>37,38</sup> PRINT particles can carry a diverse array of cargos by incorporating the cargo into the particle matrix. We have demonstrated the loading of PRINT particles with chemotherapeutics, magnetic resonance contrast agents, and fluorophores.<sup>37–40</sup> Particle surface properties can be modified by either matrix composition or post functionalization, therefore allowing particles surfaces to be amenable to functionalization with targeting moieties for targeted delivery, “stealth” PEG chains to elongate blood circulation time, or radiolabels for nuclear imaging.<sup>40–42</sup> Examples of particles made using the PRINT process are shown in Figure 2.

## 2. Nanotherapeutics

Nanoscale drug delivery vehicles are designed to improve the biodistribution and target site accumulation of systemically applied therapeutic agents. The most effective drug delivery vehicles are those that are engineered to be biocompatible, be site-specific, have optimal capability to carry relevant cargo, and demonstrate controlled release of that cargo at the pathological site. Recent work shows that exceptionally high chemotherapeutic loading is possible in poly(lactic-co-glycolic acid) (PLGA) PRINT particles.<sup>43</sup> A variety of shapes and sizes were fabricated from PLGA including cylinders, spheres, prolate ellipsoids, and toroidal particles (Figure 3).

Early systems aimed to improve site specific accumulation by means of enhanced permeation and retention passive targeting, a nonselective process that occurs due to leaky tumor vasculature that allows the accumulation of particles of a certain size at the tumor site. More advanced methods take advantage of active targeting with ligand-based carrier materials to improve target cell recognition and efficacy of drug delivery. As many cancer cells over-express the transferrin and epidermal growth factor receptors, the use of ligands specific to these receptors is an attractive targeting approach for particle based drug delivery vehicles.<sup>44,45</sup> Once the delivery vehicles reach their target, it is important that they release their cargo in a controlled fashion, and this has been accomplished through the fabrication of stimuli responsive carriers.<sup>5,46</sup> These carriers can either respond to the reducing nature of the cytosol or the decrease in pH which occurs in endosomes. These stimuli serve as triggers to break bonds between carrier and cargo or to destabilize the carrier and facilitate diffusion of its contents.

### Stimuli Responsive PRINT Carriers

A number of drug delivery platforms have taken advantage of the reductive intracellular environment by incorporating disulfide linkages into their carrier matrices, which cleave intracellularly to facilitate cargo release.<sup>46,51,52</sup> Cubic PRINT particles were fabricated with and without a reductively labile disulfide cross-linker.<sup>37</sup> Doxorubicin (Dox) was physically entrapped within the polymer matrix, and since Dox is fluorescent, its presence in the particle was confirmed using fluorescence microscopy. Dox release was monitored over 48 h for particles fabricated with either a disulfide or a triacrylate cross-linker and release was only observed for disulfide cross-linked particles incubated with dithiothreitol. The release

of Dox is due to the reduction of the disulfide bonds, which leads to a decrease in the mesh density of the polymer, making it more porous and allowing the chemotherapeutic to diffuse out. These particles were further examined for cytotoxicity in HeLa cells. Particles composed of the triacrylate cross-linker showed minimal cytotoxicity with 80% of cells remaining viable at the highest dosing.<sup>37</sup> Disulfide cross-linked particles on the other hand were effective at killing HeLa cells with merely 10% of cells remaining viable at the highest dosing, thus illustrating the activated release of Dox from the particles and the effective delivery of chemotherapeutics to HeLa cells.

In an effort to generate a series of particles with tunable cargo release characteristics, we have designed a family of novel, acid labile silyl ether cross-linkers that show exquisite control over the degradation rates.<sup>38</sup> Silyl ethers are one of the most commonly used protecting groups in organic chemistry due to the ability to adjust their reactivity by altering the alkyl substituent on the silicon atom. Generally, large or bulky substituents lead to a more stable material, whereas the addition of a small substituent leads to a material that is sensitive to acid and base. We have fabricated PRINT microparticles using bifunctional silyl ethers (BSE), specifically the dimethyl (DMS), diethyl (DES), and diisopropyl (DIS) silyl ethers which are susceptible to acid catalyzed hydrolysis and thus are ideal for the fabrication of acid sensitive biomaterials.<sup>38</sup> Cubic particles were fabricated with each BSE cross-linker and degraded under acidic conditions known to exist inside various cellular compartments. All BSE cross-linked particles preferentially degraded under acidic conditions, and the rate of degradation was accelerated as the pH decreased; however, the rate of degradation differed across the BSEs. DES particles degraded 13.6 times slower than the DMS particles, and the DIS particles were slower by 2 orders of magnitude.<sup>38</sup> This illustrates that, by changing the substituent around the silicon atom, the rate of particle degradation can be modulated. Intracellular degradation experiments were conducted with hexnut particles fabricated from the rapidly degrading DMS cross-linker and the nondegrading di-*tert*-butyl (DTS) cross-linker. Intracellular degradation of the silyl ether particles was tracked using laser confocal microscopy where the DMS particles contained a green fluorescent dye and the DTS particles contained a red fluorescent dye (Figure 4). Both particles were incubated with HeLa cells for 24 h, it is clear that after cellular internalization the DTS particles were not altered by the intracellular conditions, whereas the DMS particles exhibited signs of degradation (Figure 4). We believe that this is a promising strategy for precisely controlling the delivery of nanoparticle cargo in vivo.

### PRINT Particle Internalization and Targeting

It is well documented in the literature that cellular internalization is highly dependent on size and surface charge.<sup>47–49</sup> However, recent results indicate that particle shape also plays an important role.<sup>33,50</sup> We explored the shape effects on cellular internalization by comparing HeLa cell internalization of cubic and cylindrical PEG hydrogel particles of various sizes.<sup>28</sup> Evidence of particle internalization was obtained by flow cytometry, and confocal and transmission electron microscopy. Cubic particles were fabricated with side lengths varying from 2 to 5  $\mu\text{m}$ , and the cylindrical particles were fabricated with diameters ranging from 0.5  $\mu\text{m}$  to 200 nm, with aspect ratios ranging from 1 to 3. HeLa cells readily internalized both the cubic and cylindrical particles with dimensions as large as 3  $\mu\text{m}$ ; however, the

cylindrical particles exhibited higher internalization rates as compared to the cubic particles (Figure 5).<sup>28</sup> The internalization kinetics of the cylindrical nanoparticles by HeLa cells was dependent on aspect ratio, and particles with high aspect ratios were internalized 4 times faster than the low aspect ratio particles.

The surface charge of the particles also strongly effected internalization rates, as 84% of HeLa cells internalized at least one positively charged particle, whereas negatively charged particles were not internalized to any significant amount. One strategy for increasing the specificity of targeting was to override the negative surface charge with specific targeting ligands. We demonstrated this strategy by incubating negatively charged cylindrical PEG-based PRINT nanoparticles labeled with transferrin receptor antibody (OKT9) or human holo-transferrin (hTf) with six human tumor cell lines (HeLa, Ramos, H460, SK-OV-3, HepG2, and LNCaP) overexpressing transferrin receptor (TfR) and a transformed normal human cell line (HEK 293) with low TfR expression.<sup>42</sup> As shown in Figure 6a, internalization is indeed observed for the negatively charged particles conjugated with the targeting ligand. Targeting efficiency was found to be dependent on particle concentration, ligand density, dosing time, as well as surface receptor expression level.<sup>42</sup> After incubation for 4 h, all six tumor cell lines showed at least 80% uptake for particles labeled with either hTf or OKT9. In contrast, particles modified with control ligands showed less than 10% uptake. A kinetic study of cellular uptake was performed with four cell lines with different levels of TfR expression: Ramos > HeLa = H460 > HEK293. Not only did the uptake of PRINT particles labeled with either hTf or OKT9 increase with incubation time, but the rate clearly followed the trend of TfR expression level on the cell lines. Viability of the cells incubated with the targeted nanoparticles was evaluated, and neither the hTf nor the OKT9 labeled particles showed any appreciable toxicity to the HeLa, H460, SK-OV-3, HepG2, or LNCaP cell lines. However, both the hTf and the OKT9 labeled particles showed dose-dependent toxicity on the Ramos cell line (Figure 6b). It was suggested that the death of Ramos cells induced by the labeled nanoparticles is due to the multivalent presentation of the nanoparticle surface ligands instead of non-specific toxicity of the nanoparticles or free targeting ligand. This work demonstrates the potential of hTf and OKT9 labeled PRINT nanoparticles as a platform for targeted drug delivery to cancer cells as well as immunotherapeutic agents for B-cell lymphoma even without an added therapeutic cargo.

### Long Circulating Deformable PRINT Particles

It is well established that PEGylating the surface of nanoparticles can provide steric stabilization and confer “stealth” properties such to increase nanoparticle circulation time; however, little is known about deformability, which in biology is known to play a significant role in attenuating and controlling biodistribution.<sup>17,24,53</sup> Red blood cells are able to deform in order to navigate through various biological barriers that would prevent nonflexible objects from crossing. Some effort has been made with filomicelles to vary the modulus of micrometer sized carriers, but outside of this effort the role of deformability of carriers is essentially unexplored.<sup>21</sup> Using the PRINT technique, we were able to fabricate particles with similar size, shape, and deformability characteristics as mouse red blood cells (6  $\mu\text{m}$  in diameter).<sup>54</sup> These red blood cell mimics (RBCMs) were fabricated from hydrogels composed primarily of 2-hydroxyethyl acrylate (HEA) cross-linked with poly(ethylene



glycol) diacrylate (PEGDA). The modulus of the particles was precisely controlled by varying the amount of cross-linker. In order to track the RBCMs in vivo, a polymerizable near-IR dye was incorporated into the particle matrix (Figure 7A). Particles were administered to mice via a tail vein injection and intravital imaging was used to monitor the RBCMs real-time in the ear vasculature of the mice over a 2 h time span (Figure 7B). This data was used to calculate the circulation half-lives of the particles, based upon the change in fluorescence intensity over time. The circulation times of the particles increased with increasing particle elasticity, with the least flexible RBCMs being cleared 30 times more rapidly than the most flexible RBCMs.<sup>54</sup> A biodistribution study was conducted with the RBCMs with varying flexibility. Mice were sacrificed 2 h post injection; blood and tissue samples were harvested in order to analyze particle accumulation by fluorescence imaging. Rigid particles were found primarily in the capillary beds in the lungs, whereas the flexible particles accumulated primarily in the spleen (Figure 8).<sup>54</sup> Further studies will be required to illuminate the capability of these particles to carry and deliver therapeutic payloads; however, extremely low modulus RBCMs could have therapeutic or imaging applications for splenic disorders due to their preferential accumulation in this tissue. They also show great promise for drug delivery applications because of their long circulation times and low accumulation in the liver.

### 3. Nanoscale Contrast Agents

Nanoparticles have been explored as scaffolds for imaging probes used in the detection and monitoring of disease and disease treatment. The same characteristics that make nanoparticles an excellent platform for drug delivery make them a sought after platform for diagnostic imaging. Nanoparticle-mediated delivery of imaging probes provides an opportunity to reduce toxic side effects associated with commonly employed contrast enhancement agents by improving specific biodistribution and reducing the required dosage. Since particle-based contrast agents have the ability to carry multiple beacons per particle, they can also drastically improve the local contrast and increase sensitivity. Current research is aimed at using these particle-based contrast agents to detect, diagnose, and monitor the treatment of cancer.<sup>55,56</sup> Nanoparticle imaging probes have been used in conjunction with magnetic resonance imaging (MRI), positron emission tomography (PET), single photon emission computed tomography (SPECT), and near-infrared (NIR) fluorescence imaging.<sup>57–59</sup> Significant progress has been made in this area where nanoscale contrast agents have been used to noninvasively assess target site accumulation and to monitor the real-time biodistribution of nano-particles; however, carriers designed for imaging have almost always been spherical in shape. Therefore, the effects of carrier shape have been understudied in this field, they but have gained recent attention with MR and NIR in vivo imaging using filamentous particles.<sup>21,32</sup>

#### PRINT Contrast Agents

In recent studies, we have demonstrated the use of PRINT particles as imaging contrast agents for NIR optical, MR, and PET imaging.<sup>40,54,60</sup> By incorporating a polymerizable NIR dye within the matrix of PRINT particles, we were able to successfully track the particles in vivo using fluorescence imaging.<sup>54</sup> We also demonstrated the first examples of

shape and size specific particles for MR imaging.<sup>40</sup> We fabricated 2  $\mu\text{m}$  cubic and 200 nm cylindrical PRINT particles from a PEG hydrogel matrix containing iron oxide. Since the PRINT technique allows for the systematic control of the iron oxide content without altering the size or shape of the particles, we were able to vary the weight percent of iron oxide within the particle. From these experiments, we found that increasing the weight percent of iron oxide within the particle matrix resulted in a decrease in signal intensity in T2-weighted phantom studies,<sup>40</sup> which is common throughout the literature for MR imaging with iron oxide nanoparticles.<sup>61</sup> Park et al. recently reported that filamentous (or high aspect ratio) nanoparticles with an iron oxide core represented an improved nanomaterial platform over their spherical counterparts for targeting and imaging tumors in vivo.<sup>32</sup> We have thus begun investigating the incorporation of iron oxide into filamentous PRINT particles (Figure 9).<sup>39</sup> In contrast to encapsulating imaging agents, we were able to modify the surface of PRINT particles with <sup>64</sup>Cu, a long-lived positron emitter useful for micro-PET/CT imaging.<sup>60</sup> PRINT particles were designed with amine handles in order to covalently bind DOTA to the surface of the particles. DOTA is commonly used for binding radioisotopes to polymers and thus was used to complex <sup>64</sup>Cu to the particles.

## 4. Conclusion

As discussed in this Account, it is becoming increasingly evident that shape and modulus can have a profound effect on the behavior of delivery vehicles. Therefore, having the ability to control shape, size, matrix, surface chemistry, and modulus is crucial for designing successful delivery agents. The PRINT technique allows us to independently control all of these variables, and using this method we have created monodisperse, and size and shape specific particles for delivery of chemotherapeutics and imaging agents. Given the wide range of protocols available to modify PRINT particles, therapeutic and imaging cargos can be entrapped within the particle matrix and the exterior surfaces can be functionalized with targeting ligands or imaging agents. Future development will focus on using the PRINT platform for the codelivery of therapeutics and imaging contrast agents. In this path forward, we are currently focused on developing methods to attach stealth and/or targeting ligands to particles, as some of the compositions used for particle fabrication lack good chemical handles for surface modifications. To this end, we envision the development of a combinatorial library of shape and size specific long circulating nanoparticles that will have the ability to efficiently deliver therapeutics and imaging agents to pathological target sites.

## Acknowledgments

This work was supported in part by Liquidia Technologies, NC University Cancer Research Fund, NIH Grant U54-CA119373 and U54-CA151652 (the Carolina Center of Cancer Nanotechnology Excellence), NIH Grant 1R21HL092814 (Biomimetic Approach to the Fabrication of Red Blood Cell Mimics for Therapeutic Applications), and NIH Grant 1R01EB009565 (Engineered Organic Particles of Controlled Size, Shape and Surface Chemistry for the Programmed in vitro and in vivo Delivery of siRNA).

## References

1. Emerich DF, Thanos CG. Targeted Nanoparticle-Based Drug Delivery and Diagnosis. *J Drug Targeting*. 2007; 15(3):163–183.
2. Khemtong C, Kessinger CW, Gao JM. Polymeric Nanomedicine for Cancer MR Imaging and Drug Delivery. *Chem Commun*. 2009; 24:3497–3510.



3. Torchilin VP. Multifunctional Nanocarriers. *Adv Drug Delivery Rev.* 2006; 58(14):1532–1555.
4. McCarthy JR, Weissleder R. Multifunctional magnetic nanoparticles for targeted imaging and therapy. *Adv Drug Delivery Rev.* 2008; 60(11):1241–1251.
5. Caldorera-Moore M, Guimard N, Shi L, Roy K. Designer Nanoparticles: Incorporating Size, Shape and Triggered Release Into Nanoscale Drug Carriers. *Expert Opin Drug Delivery.* 2010; 7(4):479–495.
6. Hillebrenner H, Buyukserin F, Stewart JD, Martin CR. Template Synthesized Nanotubes for Biomedical Delivery Applications. *Nanomedicine.* 2006; 1(1):39–50. [PubMed: 17716208]
7. Gupta AK, Gupta M. Synthesis and Surface Engineering of Iron Oxide Nanoparticles for Biomedical Applications. *Biomaterials.* 2005; 26(18):3995–4021. [PubMed: 15626447]
8. Merkel TJ, Herlihy KP, Nunes J, Orgel RM, Rolland JP, DeSimone JM. Scalable Shape-Specific, Top-Down Fabrication Methods for the Synthesis of Engineered Colloidal Particles. *Langmuir.* 2010; 26(16):13086–13096. [PubMed: 20000620]
9. Moghimi SM, Hunter AC, Murray JC. Nanomedicine: Current Status and Future Prospects. *FASEB J.* 2005; 19(3):311–330. [PubMed: 15746175]
10. Liang F, Chen B. A Review on Biomedical Applications of Single-Walled Carbon Nanotubes. *Curr Med Chem.* 2010; 17(1):10–24. [PubMed: 19941481]
11. Agnihotri SA, Mallikarjuna NN, Aminabhavi TM. Recent Advances on Chitosan-Based Micro- and Nanoparticles in Drug Delivery. *J Controlled Release.* 2004; 100(1):5–28.
12. Peer D, Karp JM, Hong S, Farokhzad OC, Margalit R, Langer R. Nanocarriers as an Emerging Platform for Cancer Therapy. *Nat Nanotechnol.* 2007; 2(12):751–760. [PubMed: 18654426]
13. Samad A, Sultana Y, Aqil M. Liposomal Drug Delivery Systems: An Update Review. *Curr Drug Delivery.* 2007; 4(4):297–305.
14. Wagner V, Dullaart A, Bock AK, Zweck A. The Emerging Nanomedicine Landscape. *Nat Biotechnol.* 2006; 24(10):1211–1217. [PubMed: 17033654]
15. Zhang L, Gu FX, Chan JM, Wang AZ, Langer RS, Farokhzad OC. Nanoparticles in Medicine: Therapeutic Applications and Developments. *Clin Pharmacol Ther.* 2008; 83(5):761–769. [PubMed: 17957183]
16. Davis ME, Chen Z, Shin DM. Nanoparticle Therapeutics: An Emerging Treatment Modality for Cancer. *Nat Rev Drug Discovery.* 2008; 7(9):771–782.
17. Alexis F, Pridgen E, Molnar LK, Farokhzad OC. Factors Affecting the Clearance and Biodistribution of Polymeric Nanoparticles. *Mol Pharmaceutics.* 2008; 5(4):505–515.
18. Owens DE, Peppas NA. Opsonization, Biodistribution, and Pharmacokinetics of Polymeric Nanoparticles. *Int J Pharm.* 2006; 307(1):93–102. [PubMed: 16303268]
19. Perrault SD, Walkey C, Jennings T, Fischer HC, Chan WCW. Mediating Tumor Targeting Efficiency of Nanoparticles Through Design. *Nano Lett.* 2009; 9(5):1909–1915. [PubMed: 19344179]
20. Moghimi SM, Hunter AC, Murray JC. Long-Circulating and Target-Specific Nanoparticles: Theory to Practice. *Pharmacol Rev.* 2001; 53(2):283–318. [PubMed: 11356986]
21. Christian DA, Cai SS, Garbuzenko OB, Harada T, Zajac AL, Minko T, Discher DE. Flexible Filaments for In Vivo Imaging and Delivery: Persistent Circulation of Filomicelles Opens the Dosage Window for Sustained Tumor Shrinkage. *Mol Pharmaceutics.* 2009; 6(5):1343–1352.
22. Geng Y, Dalhaimer P, Cai SS, Tsai R, Tewari M, Minko T, Discher DE. Shape Effects of Filaments Versus Spherical Particles in Flow and Drug Delivery. *Nat Nanotechnol.* 2007; 2(4):249–255. [PubMed: 18654271]
23. Nash GB. Red-Cell Mechanics - What Changes are Needed to Adversely Affect In Vivo Circulation. *Biorheology.* 1991; 28(3–4):231–239. [PubMed: 1932715]
24. Wattendorf U, Merkle HP. PEGylation as a Tool for the Biomedical Engineering of Surface Modified Microparticles. *J Pharm Sci.* 2008; 97(11):4655–4669. [PubMed: 18306270]
25. Brannon-Peppas L, Blanchette JO. Nanoparticle and Targeted Systems for Cancer Therapy. *Adv Drug Delivery Rev.* 2009; 61(4):364–364.
26. Byrne JD, Betancourt T, Brannon-Peppas L. Active Targeting Schemes for Nanoparticle Systems in Cancer Therapeutics. *Adv Drug Delivery Rev.* 2008; 60(15):1615–1626.

27. Champion JA, Mitragotri S. Role of Target Geometry in Phagocytosis. *Proc Natl Acad Sci USA*. 2006; 103(13):4930–4934. [PubMed: 16549762]
28. Gratton SEA, Ropp PA, Pohlhaus PD, Luft JC, Madden VJ, Napier ME, DeSimone JM. The Effect of Particle Design on Cellular Internalization Pathways. *Proc Natl Acad Sci USA*. 2008; 105(33): 11613–11618. [PubMed: 18697944]
29. Muro S, Garnacho C, Champion JA, Leferovich J, Gajewski C, Schuchman EH, Mitragotri S, Muzykantov VR. Control of Endothelial Targeting and Intracellular Delivery of Therapeutic Enzymes by Modulating the Size and Shape of ICAM-1-Targeted Carriers. *Mol Ther*. 2008; 16(8): 1450–1458. [PubMed: 18560419]
30. Decuzzi P, Lee S, Bhushan B, Ferrari M. Theoretical A Model for the Margination of Particles Within Blood Vessels. *Ann Biomed Eng*. 2005; 33(2):179–190. [PubMed: 15771271]
31. Decuzzi P, Pasqualini R, Arap W, Ferrari M. Intravascular Delivery of Particulate Systems: Does Geometry Really Matter? *Pharm Res*. 2009; 26(1):235–243. [PubMed: 18712584]
32. Park JH, von Maltzahn G, Zhang LL, Schwartz MP, Ruoslahti E, Bhatia SN, Sailor MJ. Magnetic Iron Oxide Nanoworms for Tumor Targeting and Imaging. *Adv Mater*. 2008; 20(9):1630–1635. [PubMed: 21687830]
33. Champion JA, Mitragotri S. Shape Induced Inhibition of Phagocytosis of Polymer Particles. *Pharm Res*. 2009; 26(1):244–249. [PubMed: 18548338]
34. Rolland JP, Maynor BW, Euliss LE, Exner AE, Denison GM, DeSimone JM. Direct Fabrication and Harvesting of Monodisperse, Shape-Specific Nanobiomaterials. *J Am Chem Soc*. 2005; 127(28):10096–10100. [PubMed: 16011375]
35. Euliss LE, DuPont JA, Gratton S, DeSimone J. Imparting Size, Shape, and Composition Control of Materials for Nanomedicine. *Chem Soc Rev*. 2006; 35(11):1095–1104. [PubMed: 17057838]
36. Kelly JY, DeSimone JM. Shape-Specific, Monodisperse Nano-Molding of Protein Particles. *J Am Chem Soc*. 2008; 130(16):5438–5439. [PubMed: 18376832]
37. Petros RA, Ropp PA, DeSimone JM. Reductively Labile PRINT Particles for the Delivery of Doxorubicin to HeLa Cells. *J Am Chem Soc*. 2008; 130(15):5008–5009. [PubMed: 18355010]
38. Parrott MC, Luft JC, Byrne JD, Fain JH, Napier ME, DeSimone JM. Tunable Bifunctional Silyl Ether Cross-Linkers for the Design of Acid-Sensitive Biomaterials. *J Am Chem Soc*. 2010; 132(50):17928–17932. [PubMed: 21105720]
39. Nunes J, Herlihy KP, Mair L, Superfine R, DeSimone JM. Multifunctional Shape and Size Specific Magneto-Polymer Composite Particles. *Nano Lett*. 2010; 10(4):1113–1119. [PubMed: 20334397]
40. Canelas DA, Herlihy KP, DeSimone JM. Top-Down Particle Fabrication: Control of Size and Shape for Diagnostic Imaging and Drug Delivery. *Wiley Interdiscip Rev: Nanomed Nanobiotechnol*. 2009; 1(4):391–404. [PubMed: 20049805]
41. Gratton SEA, Pohlhaus PD, Lee J, Guo I, Cho MJ, DeSimone JM. Nanofabricated Particles for Engineered Drug Therapies: A Preliminary Biodistribution Study of PRINT Nanoparticles. *J Controlled Release*. 2007; 121(1–2):10–18.
42. Wang J, Tian SM, Petros RA, Napier ME, DeSimone JM. The Complex Role of Multivalency in Nanoparticles Targeting the Transferrin Receptor for Cancer Therapies. *J Am Chem Soc*. 2010; 132(32):11306–11313. [PubMed: 20698697]
43. Enlow EM, Luft JC, Napier ME, DeSimone JM. Potent Engineered PLGA Nanoparticles by Virtue of Exceptionally High Chemotherapeutic Loadings. *Nano Lett*. 2011; 11:808–813. [PubMed: 21265552]
44. Daniels TR, Delgado T, Rodriguez JA, Helguera G, Penichet ML. The Transferrin Receptor Part I: Biology and Targeting with Cytotoxic Antibodies for the Treatment of Cancer. *Clin Immunol*. 2006; 121(2):144–158. [PubMed: 16904380]
45. Daniels TR, Delgado T, Helguera G, Penichet ML. The Transferrin Receptor Part II: Targeted Delivery of Therapeutic Agents Into Cancer Cells. *Clin Immunol*. 2006; 121(2):159–176. [PubMed: 16920030]
46. Ganta S, Devalapally H, Shahiwala A, Amiji M. A Review of Stimuli-Responsive Nanocarriers for Drug and Gene Delivery. *J Controlled Release*. 2008; 126(3):187–204.

47. Rejman J, Oberle V, Zuhorn IS, Hoekstra D. Size-Dependent Internalization of Particles Via the Pathways of Clathrin-and Caveolae-Mediated Endocytosis. *Biochem J.* 2004; 377:159–169. [PubMed: 14505488]
48. Miller CR, Bondurant B, McLean SD, McGovern KA, O'Brien DF. Liposome-Cell Interactions In Vitro: Effect of Liposome Surface Charge on the Binding and Endocytosis of Conventional and Sterically Stabilized Liposomes. *Biochemistry.* 1998; 37(37):12875–12883. [PubMed: 9737866]
49. Sahay G, Alakhova DY, Kabanov AV. Endocytosis of Nanomedicines. *J Controlled Release.* 2010; 145(3):182–195.
50. Yoo JW, Doshi N, Mitragotri S. Endocytosis and Intracellular Distribution of PLGA Particles in Endothelial Cells: Effect of Particle Geometry. *Macromol Rapid Commun.* 2010; 31(2):142–148. [PubMed: 21590886]
51. Saito G, Swanson JA, Lee KD. Drug Delivery Strategy Utilizing Conjugation Via Reversible Disulfide Linkages: Role and Site of Cellular Reducing Activities. *Adv Drug Delivery Rev.* 2003; 55(2):199–215.
52. Perry JL, Guo P, Johnson SK, Mukaibo H, Stewart JD, Martin CR. Fabrication of Biodegradable Nano Test Tubes by Template Synthesis. *Nanomedicine.* 2010; 5(8):1151–1160. [PubMed: 21039193]
53. Yoo JW, Chambers E, Mitragotri S. Factors that Control the Circulation Time of Nanoparticles in Blood: Challenges, Solutions and Future Prospects. *Curr Pharm Des.* 2010; 16(21):2298–2307. [PubMed: 20618151]
54. Merkel TJ, Jones SJ, Herlihy KP, Kersey FR, Shields AR, Napier ME, Luft JC, Wu H, Zamboni WC, Wang AW, Bear JE, DeSimone JM. Using Mechano-Biological Mimicry of Red Blood Cells to Extend Circulation Times of Hydrogel Microparticles. *Proc Natl Acad Sci USA.* 2011; 108(2): 586–591. [PubMed: 21220299]
55. Bartlett DW, Su H, Hildebrandt IJ, Weber WA, Davis ME. Impact of Tumor-Specific Targeting on the Biodistribution and Efficacy of siRNA Nanoparticles Measured by Multimodality In Vivo Imaging. *Proc Natl Acad Sci USA.* 2007; 104(39):15549–15554. [PubMed: 17875985]
56. Bharali DJ, Mousa SA. Emerging Nanomedicines for Early Cancer Detection and Improved Treatment: Current Perspective and Future Promise. *Pharmacol Ther.* 2010; 128(2):324–335. [PubMed: 20705093]
57. Gambhir SS. Molecular Imaging of Cancer with Positron Emission Tomography. *Nat Rev Cancer.* 2002; 2(9):683–693. [PubMed: 12209157]
58. Cheon J, Lee JH. Synergistically Integrated Nanoparticles as Multimodal Probes for Nanobiotechnology. *Acc Chem Res.* 2008; 41(12):1630–1640. [PubMed: 18698851]
59. Hu F, Joshi HM, Dravid VP, Meade TJ. High-Performance Nanostructured MR Contrast Probes. *Nanoscale.* 2010; 2(10):1884–1891. [PubMed: 20694208]
60. Gratton SEA, Williams SS, Napier ME, Pohlhaus PD, Zhou ZL, Wiles KB, Maynor BW, Shen C, Olafsen T, Samulski ET, Desimone JM. The Pursuit of a Scalable Nanofabrication Platform for Use in Material and Life Science Applications. *Acc Chem Res.* 2008; 41(12):1685–1695. [PubMed: 18720952]
61. Sun C, Lee JSH, Zhang MQ. Magnetic Nanoparticles in MR Imaging and Drug Delivery. *Adv Drug Delivery Rev.* 2008; 60(11):1252–1265.

## Biographies

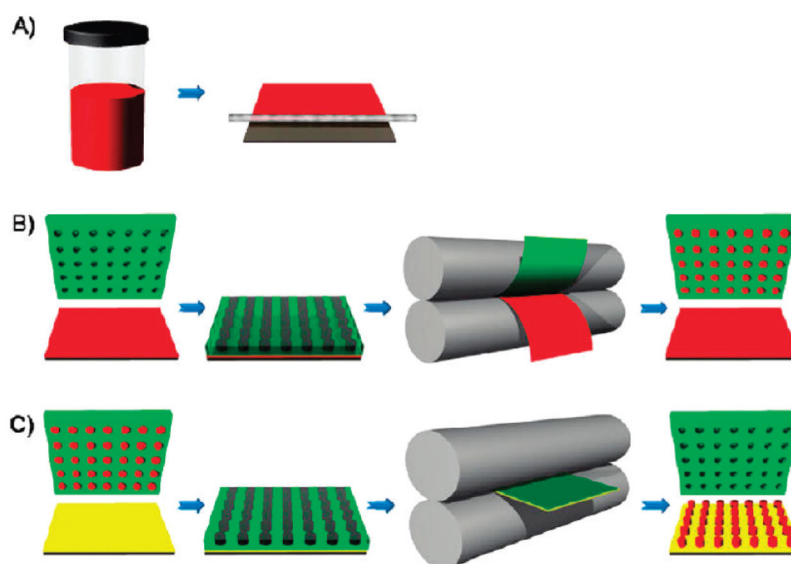
**Jillian Perry** received her B.S. in chemical engineering from the University of Florida and her Ph.D. in biomedical engineering from the University of Florida under the direction of John Stewart. She is currently a Postdoctoral Associate at the University of North Carolina at Chapel Hill under the direction of Joseph DeSimone.

**Kevin Herlihy** is a Research Associate working with Joseph DeSimone in the Department of Chemistry at the University of North Carolina at Chapel Hill and focuses on nanoparticle

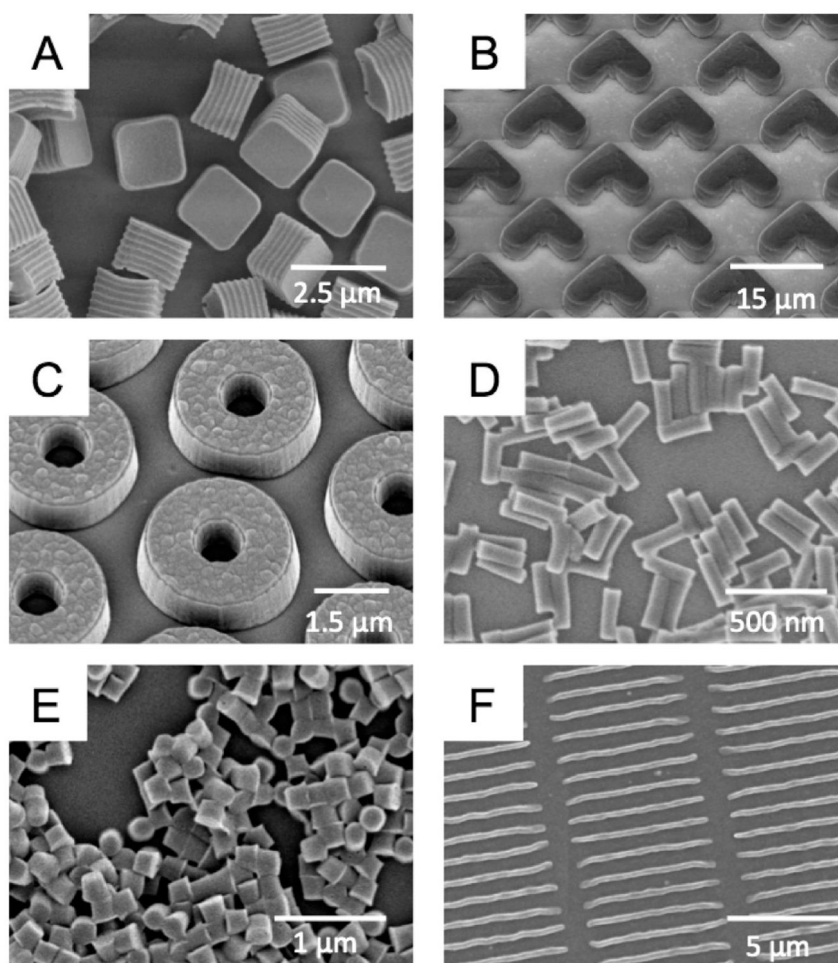
fabrication. He received his B.S. in chemistry and in environmental studies from the University of California at Santa Barbara and his Ph.D. in Chemistry from the University of North Carolina at Chapel Hill under the direction of Joseph DeSimone.

**Mary Napier** is a Senior Research Associate working with Joseph DeSimone in the Department of Chemistry at the University of North Carolina at Chapel Hill and is responsible for managing life science research projects and coordination of collaborative research efforts for the DeSimone laboratory. She received her B.S. in Chemistry from the University of Illinois, Urbana–Champaign and her Ph.D. in physical chemistry from Northwestern University. She did postdoctoral research both at Harvard University and at University of North Carolina at Chapel Hill.

**Joseph DeSimone** specializes in applying precision manufacturing approaches from the microelectronics industry for application in nanomedicine and developing new strategies for the battle against human disease. DeSimone is a fellow of the American Institute for Medical and Biological Engineering, American Association for the Advancement of Science, National Academy of Engineering, and the American Academy of Arts and Sciences. He received his B.S. in Chemistry from Ursinus College and his Ph. D. from Virginia Polytechnic Institute and State University.

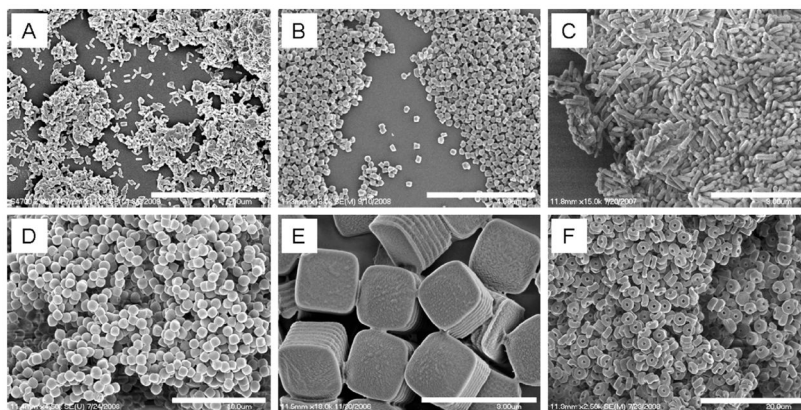
**FIGURE 1.**

Schematic illustration of the PRINT process. (A) Delivery sheet casting: A true solution (red) is made and then cast on a PET substrate using a mayer rod. Solvent is removed under heat, generating a solid state solution film referred to as the delivery sheet, as it will deliver the composition to the mold. (B) Particle fabrication: a perfluoropolyether elastomeric mold (green) is brought into contact with a delivery sheet (red), passed through a heated nip (gray), and split. The cavities of the mold are filled. (C) Particle harvesting: a filled mold is brought into contact with a high energy film or excipient layer (yellow) and passed through the heated nip without splitting. After cooling, the mold is removed to reveal an array of particles on the high-energy film or excipient layer. Reprinted with permission from ref 43. Copyright 2011 American Chemical Society.

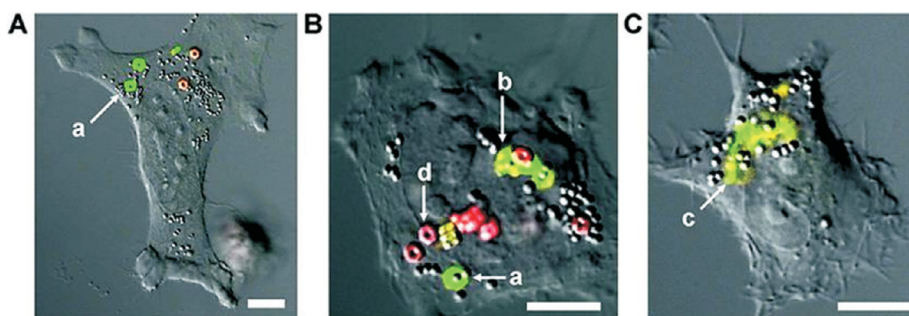
**FIGURE 2.**

Scanning electron micrograph images of particles fabricated using the PRINT method: (A) degradable 2  $\mu\text{m}$  cubic particles; (B) 10  $\mu\text{m}$  magnetic hydrogel boomerangs; (C) 3  $\mu\text{m}$  hydrogel toroids; (D) 100  $\times$  300 nm hydrogel rods; (E) 200 nm cylindrical hydrogel particles; (F) 80  $\times$  2000 nm filamentous hydrogel particles. Image (A) is reprinted with permission from ref 37, and Image (C) is reprinted with permission from ref 8. Copyright American Chemical Society 2008 and 2009. Image (E) is reprinted with permission from ref 41. Copyright 2007 Elsevier.

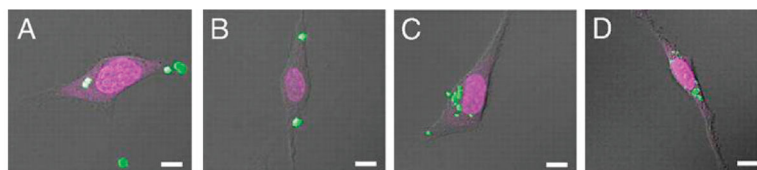


**FIGURE 3.**

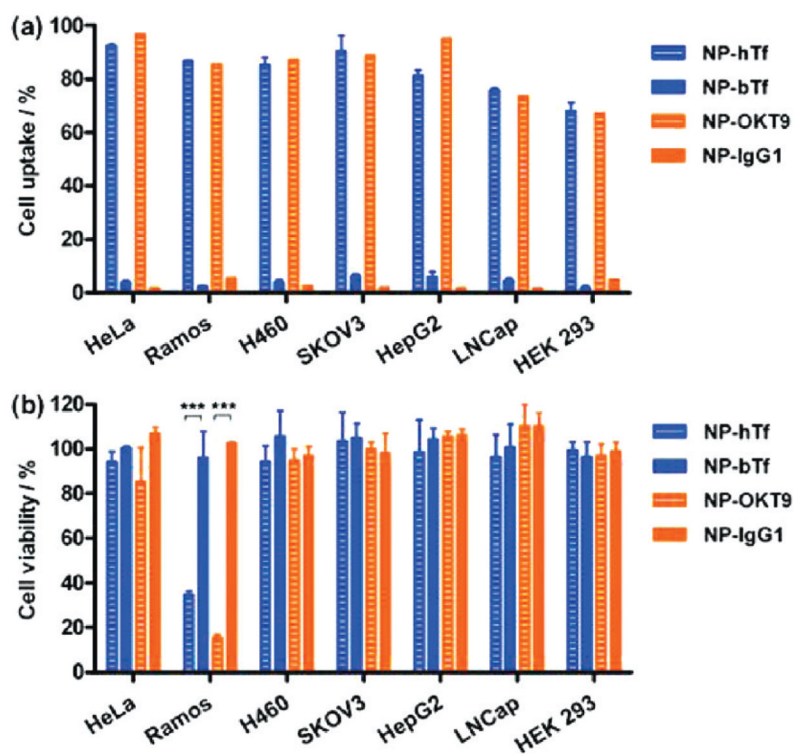
Scanning electron micrographs of PLGA PRINT particles: (A)  $80 \times 320$  nm cylinders, (B)  $200 \times 200$  nm cylinders, (C)  $200 \times 600$  nm cylinders, (D)  $1 \mu\text{m}$  sphere approximates, (E)  $2 \mu\text{m}$  cubes with ridges, and (F)  $3 \mu\text{m}$  particles with center fenestrations. Scale bars: (A)  $5 \mu\text{m}$ , (B)  $4 \mu\text{m}$ , (C)  $3 \mu\text{m}$ , (D)  $10 \mu\text{m}$ , (E)  $3 \mu\text{m}$ , and (F)  $20 \mu\text{m}$ . Reprinted with permission from ref 43. Copyright 2011 American Chemical Society.

**FIGURE 4.**

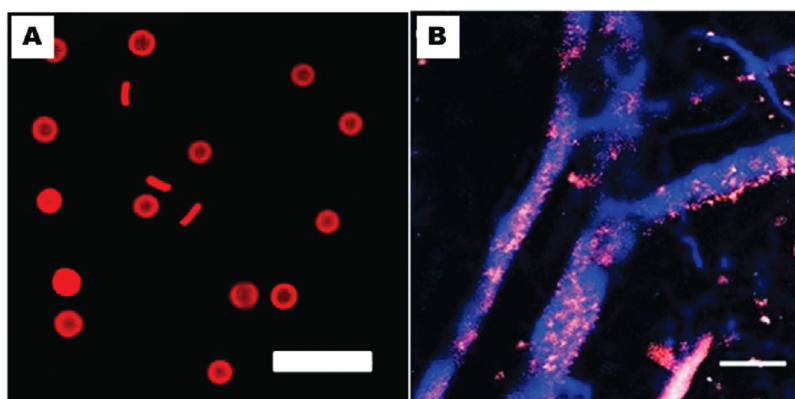
Confocal laser scanning micrographs of HeLa cells incubated with rapidly degrading hexnut particles (green) and nondegrading hexnut particles (red). Micrographs (A–C) highlight the phases of particle degradation: swelling (a), fragmentation (b), and complete degradation (c). The nondegradable particles showed no change when exposed to intracellular conditions (d). Scale bar represents 10  $\mu\text{m}$  for all images. Reprinted with permission from ref 38. Copyright 2010 American Chemical Society.

**FIGURE 5.**

Confocal laser scanning microscopy micrographs of HeLa cells after a 1 h incubation period at 37 °C with (A) 3  $\mu\text{m}$  cubic, (B) 2 m cubic, (C) 1  $\times$  1  $\mu\text{m}$  cylindrical, and (D) 200  $\times$  200 nm cylindrical particles. Scale bar represents 10  $\mu\text{m}$  in all images. Reprinted with permission from ref 28. Copyright 2008 National Academy of Science.

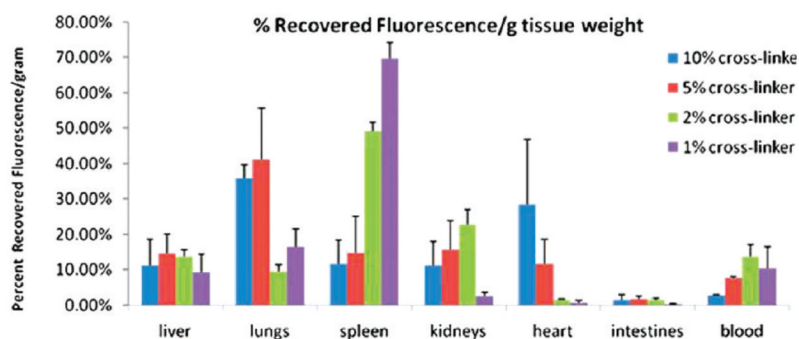


**FIGURE 6.** Transferrin receptor-targeted delivery of PRINT nanoparticles to various cancer and noncancer cell lines. (a) Cellular uptake and (b) cytotoxicity of particles. Reprinted with permission from ref 42. Copyright 2010 American Chemical Society.



**FIGURE 7.**

(A) Fluorescence micrograph of RBC mimics and (B) intravital image of blue vasculature and red particles.<sup>53</sup> Reprinted with permission from ref 54. Copyright 2011 National Academy of Science.

**FIGURE 8.**

Biodistribution of RBCMs 2 h post dosing by percent recovered fluorescence normalized for tissue weight. Error bars represent one standard deviation, with  $n = 3$  for each case.

Reprinted with permission from ref 54. Copyright 2011 National Academy of Science.



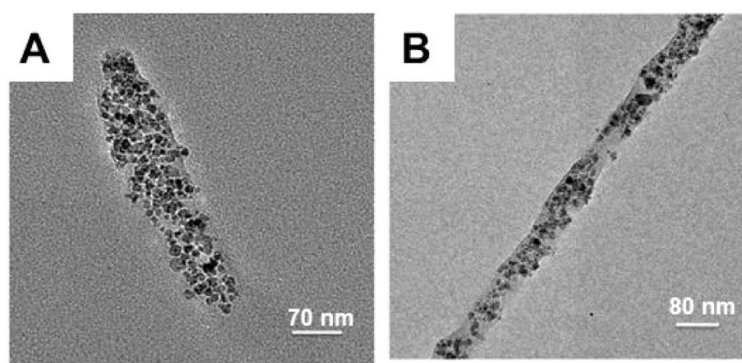


**FIGURE 9.**

Transmission electron microscopy images of PRINT particles (A)  $80 \times 320$  nm and (B)  $80 \times 2000$  nm containing iron oxide nanoparticles. Reprinted with permission from ref 39. Copyright 2010 American Chemical Society.